Turkish Journal of Electrical Engineering & Computer Sciences

http://journals.tubitak.gov.tr/elektrik/

Research Article

Turk J Elec Eng & Comp Sci
(2019) 27: 1908 – 1921

doi:10.3906/elk-1803-101

Channel estimation for OFDM-IM systems

Yusuf ACAR[1,2,*], **Sultan ALDIRMAZ ÇOLAK**[3], **Ertuğrul BAŞAR**[4]

[1]Department of Electrical and Electronics Engineering, Faculty of Engingeering, İstanbul Kültür University, İstanbul, Turkey

[2]Wireless Technology Center, Purdue University, Fort Wayne, Indiana, USA

[3]Department of Electronics and Communication Engineering, Faculty of Engineering, Kocaeli University, Kocaeli, Turkey

[4]Department of Electronics and Communication Engineering, Faculty of Electrical and Electronics Engineering, İstanbul Technical University, İstanbul, Turkey

Received: 15.03.2018 • **Accepted/Published Online:** 19.02.2019 • **Final Version:** 15.05.2019

Abstract: Orthogonal frequency division multiplexing with index modulation (OFDM-IM) has been recently proposed to increase the spectral efficiency and improve the error performance of multicarrier communication systems. However, all the OFDM-IM systems assume that the perfect channel state information is available at the receiver. Nevertheless, channel estimation is a challenging problem in practical wireless communication systems for coherent detection at the receiver. In this paper, a novel method based on the pilot symbol-aided channel estimation technique is proposed and evaluated for OFDM-IM systems. Pilot symbols, which are placed equidistantly, allow the regeneration of the response of the channel so that pilot symbol spacing can fulfill the sampling theorem criterion. Our results shows that the low-pass interpolation and SPLINE techniques perform the best among all the channel estimation algorithms in terms of bit error rate and mean square error performance.

Key words: Channel estimation, orthogonal frequency division multiplexing, indices modulation, frequency selective fading channel, interpolation

1. Introduction

Orthogonal frequency division multiplexing (OFDM) is a backbone of many wireless communications standards such as IEEE 802.16, WiMAX, and LTE; furthermore, it has also been adopted for both uplinking and downlinking of 5G New Radio. One of the most important reasons for the preference of OFDM is its property of converting frequency-selective channels into flat fading by dividing the wideband into smaller subbands. Another popular system, multiinput multioutput (MIMO) transmission, has a major role in 4G (LTE) systems. In an LTE system, MIMO and OFDM are used together in order to increase the data rate. However, this data rate does not seem to be sufficient for next-generation systems. To provide better data rates and high spectral efficiency, Mesleh et al. proposed the scheme of spatial modulation (SM). SM uses active antenna indices to transmit bits in addition to conventional modulations. SM can be considered as a low complexity alternative to conventional MIMO transmission schemes [1]. By using this technique, some drawbacks of the conventional MIMO systems, such as operation with multiple radio frequency chains, interantenna synchronization (IAS) at the transmitter, and interchannel interference (ICI) at the receiver, can be circumvented [2–4].

*Correspondence: y.acar@iku.edu.tr, acary@pfw.edu

Recently, Basar et al. proposed the OFDM-IM scheme [5]. OFDM and SM schemes have been brought together in this technique, maintaining the properties of both. Similar to the use of active antenna indices for extra bit transmission in SM, OFDM-IM also uses indices of subcarrier locations to transmit data. Thus, average bit error probability (ABEP) of OFDM-IM under frequency-selective channels is better than the classical OFDM [6, 7]. Furthermore, it requires less power compared to OFDM under the same spectral efficiency to achieve a target error rate. The use of indices for transmission adds a new dimension (third dimension) to the two-dimensional signal space. One of the main contributions of the OFDM-IM system is the use of subcarrier indices as a data source. For this reason, OFDM-IM appears as a promising next-generation wireless communication technique, which offers a balanced trade-off between system performance and spectral efficiency compared to the classical OFDM system. OFDM-IM has attracted tremendous attention in the past few years. Interested readers are referred to [6, 7] and the references therein for an overview of the most recent developments.

Despite its aforementioned advantages, there are still problems in the practical application of OFDM-IM in wireless communications. The OFDM-IM receiver has to detect both the transmitted symbol and the indices of active subcarriers. In [5], detection of both active subcarriers indices and symbols was realized by using maximum likelihood (ML) and log likelihood ratio (LLR) detection methods under the assumption that the receiver has perfect channel state information (P-CSI). However, this assumption is impossible for practical systems, even if high computational complexity channel estimation techniques are used at the receiver. Consequently, there would always be a performance gap between the practical case and the perfect CSI assumption. Therefore, channel estimation is an essential process at the practical OFDM-IM receiver during the coherent detection of the transmitted symbols and the active subcarrier, which are randomly selected. To reduce the performance gap, channel estimation techniques with low computational complexity should be developed. Recently, channel estimation has been comprehensively studied in the literature for SM-based systems [8–10]. However, to the best of our knowledge, the channel estimation problem of the OFDM-IM has not been studied in the literature yet.

In the literature, a considerable number of studies on channel estimation for OFDM systems, particularly comb-type based structures, can be found. Pilot-assisted channel estimation (PSA-CE) has generally been performed for coherent detection performance in wireless environments and has been adapted in various communication systems, such as LTE-Advanced and WIMAX systems [11, 12]. However, when the indices of the subcarriers are activated according to the corresponding information bits, the pilot symbol sequence will not be effective to implement channel estimation efficiently. Therefore, these techniques cannot be applicable directly to OFDM-IM due to subcarrier activation that depends on the indices bits. In this paper, we propose a new PSA-CE technique with interpolation for OFDM-IM systems according to activated subcarriers. First, pilot symbols are inserted with regard to activated subcarriers in the frequency domain to track the variation of the channel in the frequency domain. Then one of the interpolation techniques, such as nearest interpolation (NI), piecewise linear interpolation (PLI), piecewise cubic Hermite (PCHIP, SPLINE), FFT interpolation (FFTI), and low-pass interpolation (LPI), is performed to estimate the channel frequency responses at data symbols. With extensive computer simulations, it is demonstrated that the LPI and SPLINE techniques perform the best among all the channel estimation algorithms in terms of bit error rate (BER) and mean square error (MSE) performance. Moreover, classical OFDM results are given as a benchmark. It is shown that OFDM-IM is more robust to channel estimation errors than classical OFDM systems.

The main contributions of the paper are summarized as follows:

- In the literature, most of the studies on OFDM-IM present the performance of the system model assuming that the receiver has perfect CSI knowledge. However, this assumption is not practical. To present the real performance of the OFDM-IM system, channel estimation is indispensable. This paper analyzes this problem for the first time in the literature.
- BER performance of different interpolation techniques, such as NI, PLI, PCHIP, SPLINE, FFTI, and LPI, are investigated for the OFDM-IM system.
- MSE performance of the aforementioned interpolation techniques are investigated for the OFDM-IM system.

The paper is organized as follows. Section 2 provides some essential information of OFDM-IM systems and the detection process. Section 3 gives a short overview about channel estimation for the OFDM-IM system. Section 4 provides brief information about interpolation techniques. Then the proposed pilot-assisted channel estimation is investigated. Computer simulation results are given and discussed in Section 5. Finally, our paper concludes in Section 6.

Throughout the paper, the following notation and assumptions are used. Small and bold letters '$\mathbf{a}$' denote vectors. Capital and bold letters '$\mathbf{A}$' denote matrices. $(.)^T$, $(.)^H$, $\|.\|$, and $(.)^{-1}$ denote transpose, Hermitian transpose, Euclidean norm, and inverse of a vector or a matrix, respectively. S denotes the complex signal constellation of size M. The probability density function (PDF) of the random variable (r.v.) x denoted by $p_X(x)$ and $E\{X\}$ represents expectation of the r.v. X.

2. Orthogonal frequency division multiplexing-index modulation (OFDM-IM)

2.1. Signal model

In this paper, we analyze an OFDM-IM system operating over a frequency-selective Rayleigh fading channel. The data structure of the classical OFDM symbol and OFDM-IM symbol is given in Figure 1 and the parameters of the OFDM-IM scheme are summarized in the Table.

In the OFDM-IM scheme, the total transmitted bits are split into g subblocks and there are index selectors and mapping blocks for each subblock. Then, at each subblock β, indices are selected by using the incoming p_1 bits at the index selector. The selected indices are given as $I_\beta = \{i_{\beta,1} \cdots i_{\beta,k}\}$ where $i_{\beta,\gamma} \in [1, \ldots, n]$ for $\beta = 1, \ldots, g$ and $\gamma = 1, \ldots, k$. The data symbols at the output of the M-ary modulator, which are determined by p_2 bits, are given as $\boldsymbol{s}_\beta = [s_\beta(1) \cdots s_\beta(k)]$ where $s_\beta(\gamma) \in S, \beta = 1, \ldots, g, \gamma = 1, \ldots, k$. By using I_β and s_β for all β, the OFDM block generator creates all of the subblocks and then creates an $N \times 1$ OFDM-IM symbol as $\boldsymbol{x}_F = [x(1) \cdots x(N)]^T$ where $x(\alpha) \in \{0, S\}, \alpha = 1, \ldots, N$. The OFDM-IM symbol contains some zero terms whose positions carry information, unlike the conventional OFDM.

The transmission frequency-selective channel is assumed as a Rayleigh fading channel whose channel coefficients can be written as

$$\boldsymbol{h}_T = [h_T(1) \cdots h_T(d)]^T, \tag{1}$$

whose elements are complex Gaussian random variables with distribution $\mathbb{CN}(0, \frac{1}{d})$ and d is the length of the channel impulse response (CIR). At the trasmitter, after IFFT operation, a cyclic prefix (CP) is added to the output of the IFFT. Then OFDM-IM signal is sent over the channel $\boldsymbol{h}_T$.

At the receiver, after using an A/D converter and removing the CP, fast Fourier transform (FFT) is applied to the received OFDM-IM symbol. The received frequency domain OFDM-IM symbol can be written

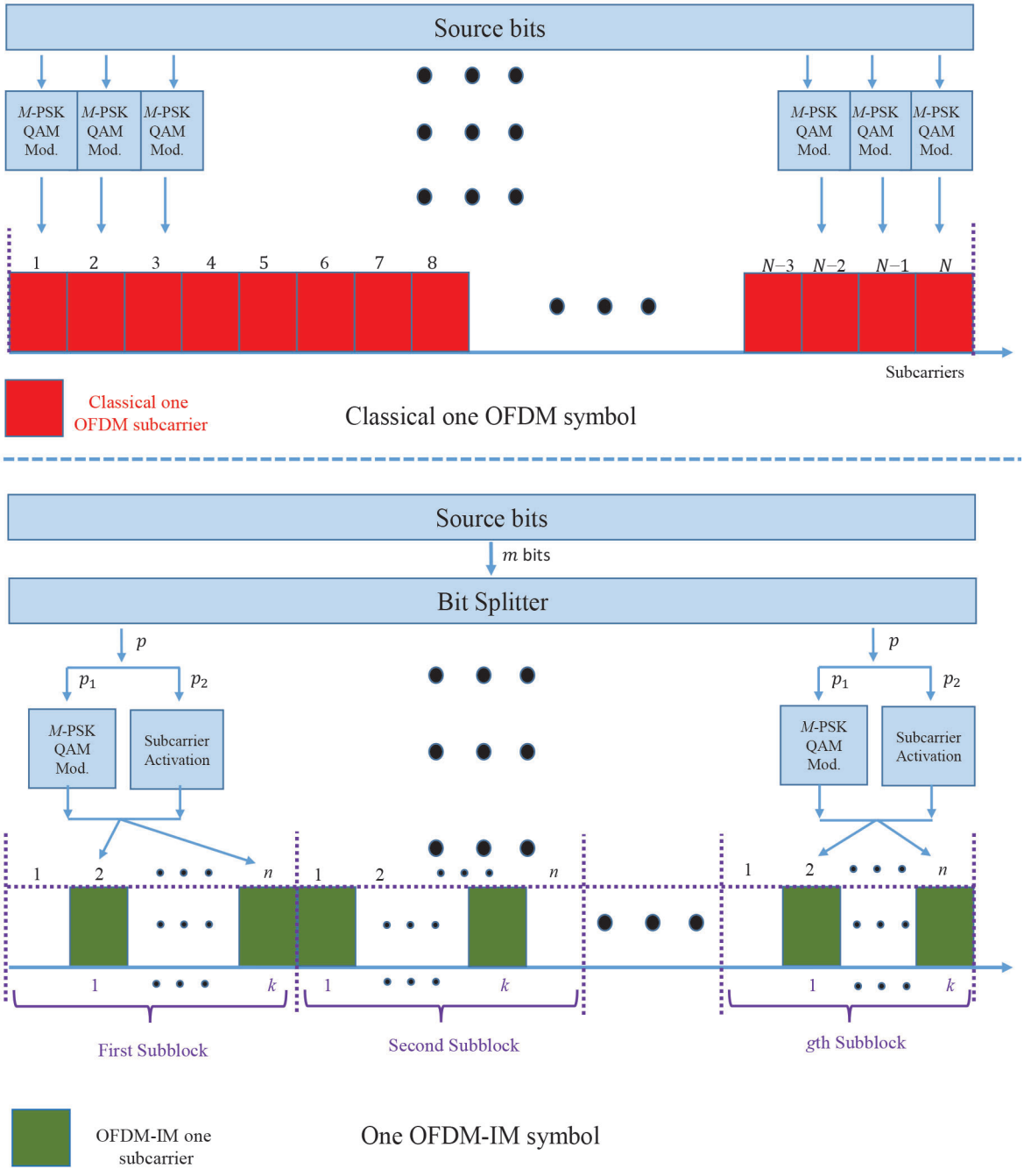

Figure 1. Data frame structure of conventional OFDM and OFDM-IM.

for the fth subcarrier as follows:

$$y_F(f) = h_F(f)x(f) + w_F(f), \quad f = 1, ..., N, \tag{2}$$

where $w_F(f)$ and $h_F(f)$ are the frequency-domain noise samples and channel fading coefficients with distributions $\mathcal{CN}(0,1)$ and $\mathcal{CN}(0, \left(\frac{K}{N}\right) W_{0,T})$, respectively, and $W_{0,T}$ is the time domain noise variance.

Table. OFDM-IM parameters.

Parameters	Definition
g	Number of subblocks
m	Total number of information bits for OFDM-IM symbol
p	Number of bits transmitted in each subblock (i.e. $p = m/g$)
N	Number of OFDM subcarriers (i.e. size of FFT)
n	OFDM-IM subblock length (i.e. $n = N/g$)
k	Number of activated subcarrier indices in each subbock
K	Total number of active subcarriers (i.e. $K = kg$)
p_1	Total number of bits that are mapped onto the active indices in each subbock
p_2	Total number of bits that are mapped onto the M-ary signal constellation

2.2. Detection in OFDM-IM system

In the OFDM-IM scheme, the receiver should detect the indices of the active subcarriers besides the information bits carried by the M-ary symbols. In [5], maximum likelihood (ML) and log likelihood ratio (LLR) detectors were proposed. The ML detector performs all subblock realizations by considering a search for all transmitted symbols and subcarrier index combinations as follows:

$$\left(\hat{I}_\beta, \hat{s}_\beta\right) = \arg\min_{I_\beta, s_\beta} \sum_{\gamma=1}^{k} |y_F^\beta(i_{\beta,\gamma}) - h_F^\beta(i_{\beta,\gamma}) s_\beta(\gamma)|^2, \tag{3}$$

where $y_F^\beta(\xi) = y_F(n(\beta-1)+\xi)$ and $h_F^\beta(\xi) = h_F(n(\beta-1)+\xi)$ are the corresponding fading coefficients and received signals, respectively.

It is shown that the complexity of ML decoding increases for higher n and k values [5]. To reduce the encoder/decoder complexity, in this work, the LLR algorithm is utilized at the receiver to decide the most likely corresponding data symbols and active subcarriers. It determines the logarithm of the ratio of a posteriori probabilities of OFDM samples for each subcarrier. This ratio is given as:

$$\lambda(f) = \ln \frac{\sum_{\chi=1}^{M} P(x(f) = s_\chi \,|y_F(f))}{P(x(f) = 0 \,|y_F(f),)} \tag{4}$$

where $s_\chi \in S$. As seen from Eq. (4), the higher value of $\lambda(f)$ indicates that the fth subcarrier is more likely to be active. Finally, active indices and symbols are then passed to the demapper to retrieve the original information. As a result, in Eqs. (3) and (4), the indices of the active subcarriers and symbol detection are performed under the assumption that P-CSI is perfectly known at the receiver. However, it is challenging to obtain P-CSI for practical systems. Therefore, channel estimation is an important and essential process at the practical OFDM-IM receiver for the coherent detection of s_β and I_β.

3. Channel estimation for the OFDM-IM system

Generally, wireless communications systems are exposed to frequency selective fading channel due to the multipath propagation. Therefore, the channel may be destructive for the transmitted signal. To compensate the channel effects, the channel frequency response should be estimated on the receiver side. Besides, some systems such as OFDM-IM need the channel frequency response at the receiver side for joint detection of the modulated symbols, s_β, and the subcarrier indices, I_β. However, to the best of our knowledge, channel estimation problems have not been extensively explored for OFDM-IM in the literature yet. In OFDM-IM

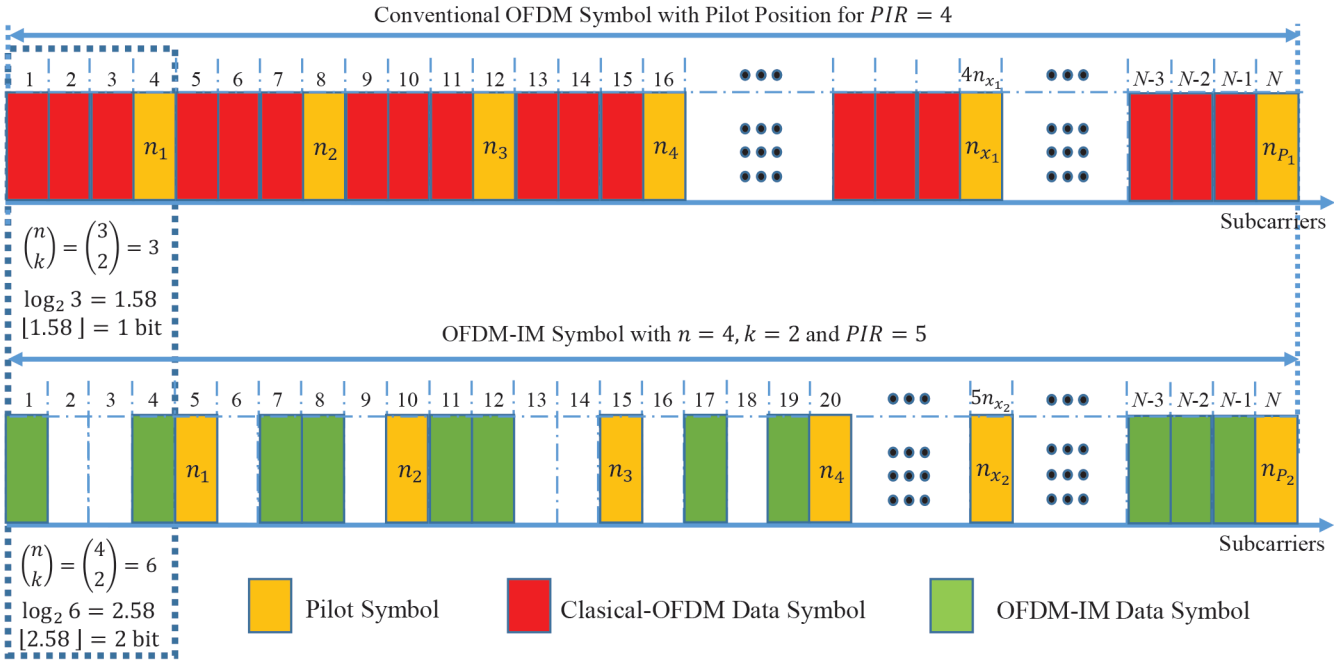

Figure 2. Pilot frame structure of conventional OFDM and OFDM-IM.

systems, when the subcarriers are activated according to the associated data bits, the pilot symbol sequence cannot be effectively implemented for channel estimation.

The top of Figure 2 shows the well known comp-type frame structure of the conventional OFDM technique. In this figure, yellow, red, and green items represent the pilot symbol, classical OFDM data symbol, and OFDM-IM data symbols, respectively. It is clear that conventional OFDM systems do not convey information bits over the subcarrier indices; hence, the positions of the pilots are not important at the transmitter and the pilots can be placed without any restriction. The bottom of Figure 2 shows the proposed frame structure for OFDM-IM systems. As shown in this figure, the main difference between these structures is that in the conventional OFDM system, all subcarriers are activated; however, in the OFDM-IM system, this is not the case. Hence, the positions of pilots become important for OFDM-IM systems. Therefore, in Figure 2, the pilot positions have been taken into account in the proposed structure of the OFDM-IM system. For example, in classical OFDM, when the pilot insertion rate (PIR) is chosen as 3, the pilot positions will be $\{4-8-12-16-\cdots N\}$. In that case, only one (i.e. $\log_2(PIR-1) = 1.58$)) index bit can be transmitted by OFDM-IM with $n = 4$ because the total number of active subcarrier combinations is two in each subblock (i.e. the second and the third subcarriers between consecutive pilot tones can be used for IM). As a result, PIR is more important for OFDM-IM systems. In our proposed PSA-CE technique with interpolation, we take into account the activated subcarriers and PIR.

To obtain the frequency variation of the wireless channel, pilot symbols (where totally P pilot symbols are employed) are placed with equal distances in the frequency domain. Then the received signals at pilot subcarriers can be expressed for each OFDM symbol as follows:

$$y_F(n_p) = \psi h_F(n_p) + w_F(n_p), n_p = 1, PIR+1, ..., N, \tag{5}$$

where ψ is the pilot symbol. After obtaining the received signal at the known pilot tone positions, the frequency

response of the channel at the pilot position can be estimated by using the least square (LS) method as follows:

$$\widehat{h}(n_p) = y_F(n_p)/\psi. \tag{6}$$

Curve fitting or interpolation techniques can be used in the process of constructing the whole channel response. In this paper, the following interpolation techniques are used to estimate the channel variations at the data subcarriers by using the channel parameters in Eq. (6).

4. Interpolation techniques

In this paper, in order to track the selectivity of channels, we use suitable interpolation techniques. Hence, the channel variations at the data subcarriers are estimated by interpolation methods. Coleri et al. studied several interpolation techniques comparatively, and they showed that the LPI has advantages compared to the others due to its superior performance [13]. In the following subsection, we give some brief information about different interpolation methods.

4.1. Piecewise linear interpolation (PLI)

Due to its inherent simplicity and easy implementation, PLI is one of the most favorable interpolation methods [14]. PLI can be expressed for $p = 1, 2, \cdots, P$ as follows:

$$h(n) \;=\; \hat{h}(n_p) + \left(\hat{h}(n_{p+1}) - \hat{h}(n_p)\right)\left(\frac{n-n_p}{D}\right), \text{for } n_p \le n \le n_{p+1}, \tag{7}$$

where $\hat{h}(n_p)$ and $h(n)$ are the estimated CIRs at pilot positions and at all data positions, respectively.

4.2. Piecewise cubic Hermite interpolation

The piecewise cubic polynomials are among the powerful solutions for interpolation [15, 16].

Eq. (8) represents the piecewise cubic Hermite interpolation for the local variables $m = n - n_p$ on the interval $n_p \le n \le n_{p+1}$:

$$h(n) = \frac{3Dm^2 - 2m^3}{D^3}\hat{h}(n_{p+1}) + \frac{D^3 - 3Dm^2 + 2m^3}{D^3}\hat{h}(n_p) + \frac{m^2(m-D)}{D^2}d_{p+1} + \frac{m(m-D)^2}{D^2}d_p, \tag{8}$$

where d_p is the slope of the interpolant at n_p and D denotes the length of the subinterval. There are numerous approaches to assess both the function values and the first derivatives at the positions of a set of data points. Hence, the slope d_p should be calculated in a proper way. In what follows, we introduce the *pchip* and *spline* interpolation techniques to acquire piecewise cubic Hermite interpolation.

4.2.1. Shape-preserving piecewise cubic interpolation (PCHIP)

The PCHIP algorithm determines the slopes d_p as follows [17, 18]:

- Assume that $\delta_p = \frac{\hat{h}(n_{p+1}) - \hat{h}(n_p)}{D}$ is the first-order difference of $\hat{h}(n_p)$.
- If δ_p and δ_{p-1} have opposite signs, set $d_p = 0$.

- If δ_p and δ_{p-1} have zero or both of them have zero signs, set $d_p = 0$.
- Otherwise, set d_p as $d_p = \frac{2\delta_{p-1}\delta_p}{\delta_{p-1}+\delta_p}$.

4.2.2. Cubic SPLINE interpolation

The common property of PCHIP and this technique is that they have the same interpolation constraints. The cubic SPLINE algorithm employs low-degree polynomials in each interval and selects the polynomial pieces. This technique is twice continuously differentiable. This interpolation method can calculate the d_p values as follows [19]:

$$\mathbf{Bd} = \mathbf{r}, \tag{9}$$

where $\mathbf{d} = [d_0, d_1, \ldots, d_{P-1}]^T$ is the slopes vector and $\mathbf{B}$ is a tridiagonal matrix:

$$\mathbf{B} = \begin{bmatrix} A & 2A & & & & & \\ A & 4A & A & & & & \\ & A & 4A & A & & & \\ & & \ddots & \ddots & \ddots & & \\ & & & A & 4A & A & \\ & & & & A & 4A & \end{bmatrix}$$

, and the right-hand side of Eq. (9) is $\mathbf{r} = 3\left[\frac{5}{6}A\delta_0 + \frac{1}{6}A\delta_1, A\delta_0 + A\delta_1, \ldots, A\delta_{P-3} + A\delta_{P-2}, \frac{1}{6}A\delta_{P-3} + \frac{5}{6}A\delta_{P-2}\right]^T$.

As a conclusion, the SPLINE interpolant is smoother than the PCHIP interpolant. While PCHIP has only first continuous derivatives that imply a discontinuous curvature, in addition to the first continuous derivatives, SPLINE also has a second continuous derivative. On the other hand, contrary to PCHIP, SPLINE might not be protected to preserve the shape.

4.3. Low pass interpolation (LPI)

The LPI technique is another method for channel estimation [20]. For the calculation of the filter coefficients, LPI does not require the knowledge of the SNR as well as the autocorrelation function of the channel fading coefficients. First, $Z-1$ zeros are inserted between successive samples of $\hat{h}(n_p)$ with a sampling rate f_p, as:

$$\tilde{h}(n) = \begin{cases} \hat{h}(n_p) & n = 0 : Z : Z(P-1) \\ 0 & \text{otherwise.} \end{cases} \tag{10}$$

Then, to calculate the interpolated signal $h(n)$, Eq. (10), and the raised-cosine low-pass filter $h_{LP}(n)$ with a cutoff frequency, specified by $f_c = \frac{\tilde{f}_p}{2Z} = \frac{f_p}{2}$, we have the following [21]:

$$h(n) = \sum_{n_p=-\infty}^{\infty} h_{LP}(n - n_p)\tilde{h}(n). \tag{11}$$

4.4. Fast Fourier transform interpolation (FFTI)

The FFT algorithm is an accurate and efficient method for interpolation and a well-known application of the FFT [22, 23]. This technique is also very effective by significantly reducing the noise on the estimated channel coefficients [24].

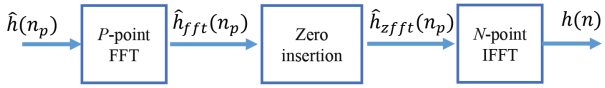

Figure 3. The block diagram of the FFT interpolator.

Figure 3 shows the basic block diagram of the FFT interpolator. As shown in Figure 3, after obtaining channel parameters at the pilot tones sequence, FFT of $\hat{h}(n_p)$ is computed as $\hat{h}_{fft}(n_p)$. Secondly, the null samples are added in $\hat{h}_{fft}(n_p)$ to obtain $\hat{h}_{zfft}(n_p)$. Finally, the inverse FFT (IFFT) is applied to the oversampled vector, $\hat{h}_{zfft}(n_p)$, to calculate the interpolated signal $h(n)$.

4.5. Zero-order hold or nearest interpolation (NI)

NI is one of the simplest interpolation techniques in which the value of the nearest point is selected. To calculate the interpolated signal $h(n)$, Eq. (10) is convolved with $h_Z(n)$ as given in the following, where $h_Z(n)$ is equal to 1 for $0 \leq n \leq Z$ and zero otherwise:

$$h(n) = \sum_{n_p=-\infty}^{\infty} h_Z(n - n_p)\tilde{h}(n_p), \tag{12}$$

where Z denotes the length of the subinterval.

5. Simulation results

The BER and MSE performance of OFDM-IM systems is evaluated by employing OFDM-IM with different N, k, and n parameters under frequency-selective Rayleigh channels. Monte Carlo simulations are performed by employing BPSK, QPSK, 8-QAM, and 16-QAM signal constellations. Moreover, we present channel estimation results for classical OFDM systems under the same spectral efficiency with OFDM-IM systems. In all computer simulations, we assume the following system parameters: $d = 10$ and a CP length of $L = 16$. The signal-to-noise ratio (SNR) is defined as E_s/N_0, where E_s is energy per symbol and N_0 is the noise power. At the receiver, an LLR detector is used for the detection process.

In Figures 4a and 4b, the BER performances of the proposed interpolation techniques are compared for BPSK signaling with $n = 4$, $k = 2$, and $PIR = 5$ where PIR is pilot insertion rate. As seen from Figure 4a, for $N = 128$, all interpolation-based channel estimation techniques have an irreducible error floor at high SNR values. To overcome this problem, PIR might be decreased; however, the overhead increases in this case and the spectral efficiency of OFDM-IM decreases due to the reduced number of active subcarrier combinations. Therefore, in Figure 4b, we increased the total number of the subcarriers to $N = 256$. It is observed that SPLINE slightly outperforms FFTI while it shows a similar performance to LPI for the scheme with $N = 256$, $n = 4$, $k = 2$, and $PIR = 5$. Moreover, SPI and LPI exhibit a detection gain of about 6 dB over PCHIP at a BER value of 10^{-4}. It is also demonstrated that NI, LI, and PCHIP have an irreducible error floor at high SNR. Moreover, as seen in this figure, OFDM-IM is more robust to channel estimation errors than classical OFDM systems.

BER performance results of QPSK and 8-QAM signaling with $n = 4$, $k = 2$, $PIR = 5$, and $N = 256$ are plotted in Figures 5a and 5b as a function of SNR. In Figure 5a, SPLINE and LPI have the same BER performances and they perform better than the other interpolation-based channel estimation techniques. It is

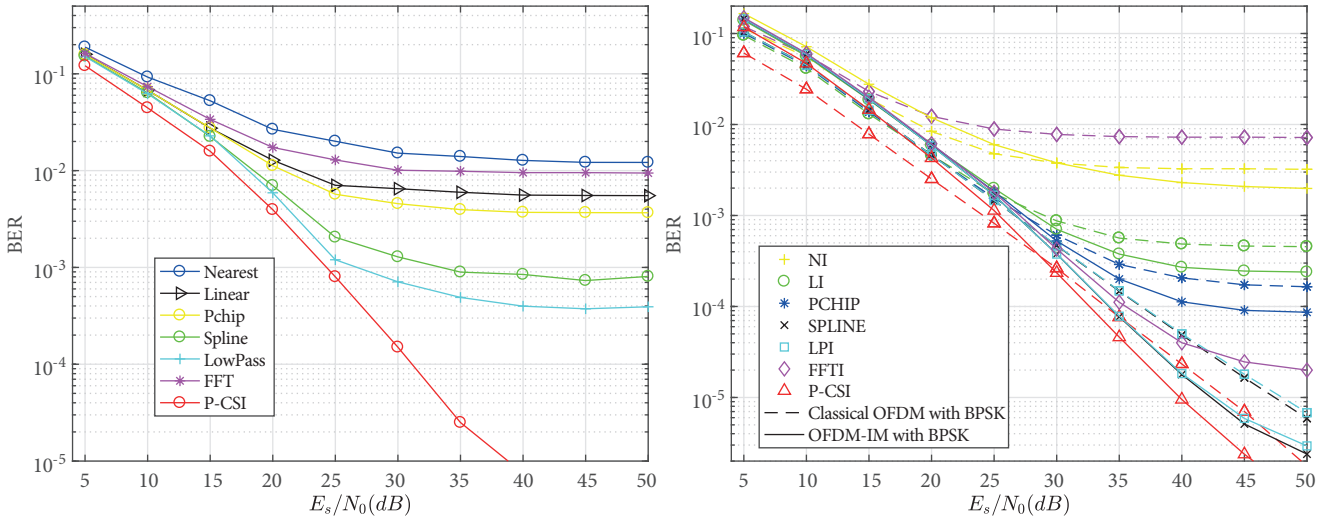

Figure 4. The BER performance of OFDM-IM with BPSK, $n = 4$, $k = 2$, $PIR = 5$: (a) $N = 128$, (b) $N = 256$.

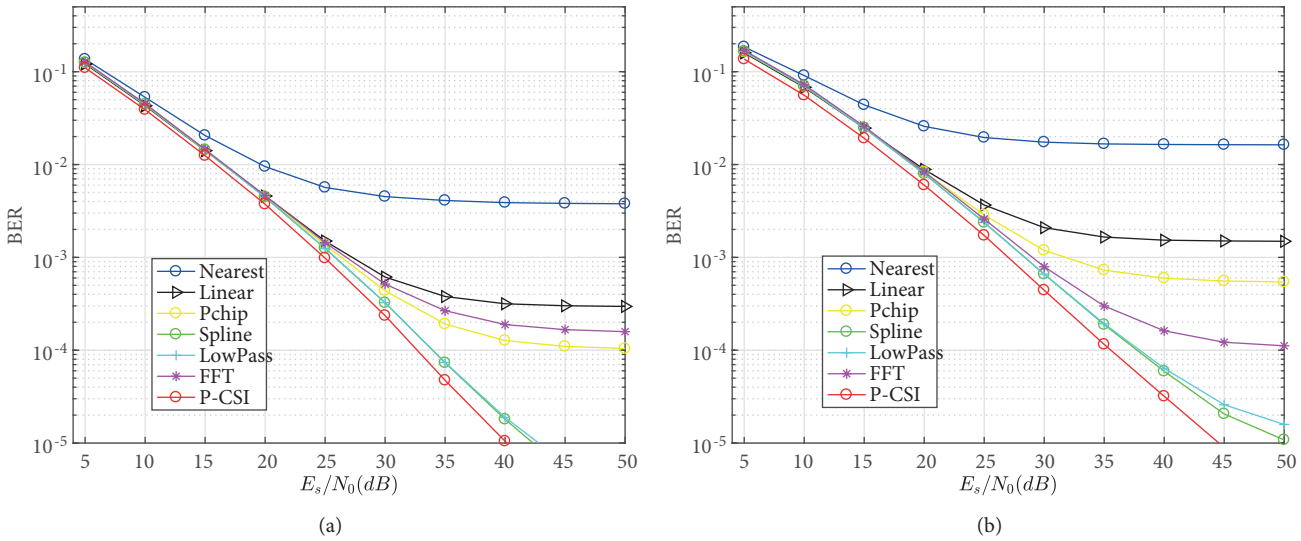

Figure 5. The BER performance of OFDM-IM with $n = 4$, $k = 2$, $PIR = 5$, $N = 256$: (a) QPSK, (b) 8-QAM.

also shown that NI, PLI, PCHIP, and FFTI-based channel estimation methods have an irreducible error floor at high SNR. The superiority in performance of SPLINE interpolation over LPI is illustrated in Figure 5b at high SNR for 8-QAM signaling. It is seen from Figure 5b that SPLINE and LPI exhibit a detection gain of about 8 dB over FFTI at a BER value of 10^{-4}.

Pilot overhead is one of the problems faced in receiver design. It decreases the efficiency and data rate of systems. To overcome this problem, we decrease the number of the pilot symbols, i.e. we increase PIR. In Figures 6a and 6b, the BER performances of the proposed interpolation techniques are compared for QPSK and 8-QAM signaling with $n = 8$, $k = 2$, and $PIR = 9$. The BER performances of the channel estimation algorithms based on SPLINE and LPI are considerably better than the NI, LI, PCHIP, and FFTI algorithms, while these also yield an error floor at high SNRs. In particular, in Figure 6b, it is observed that LPI and

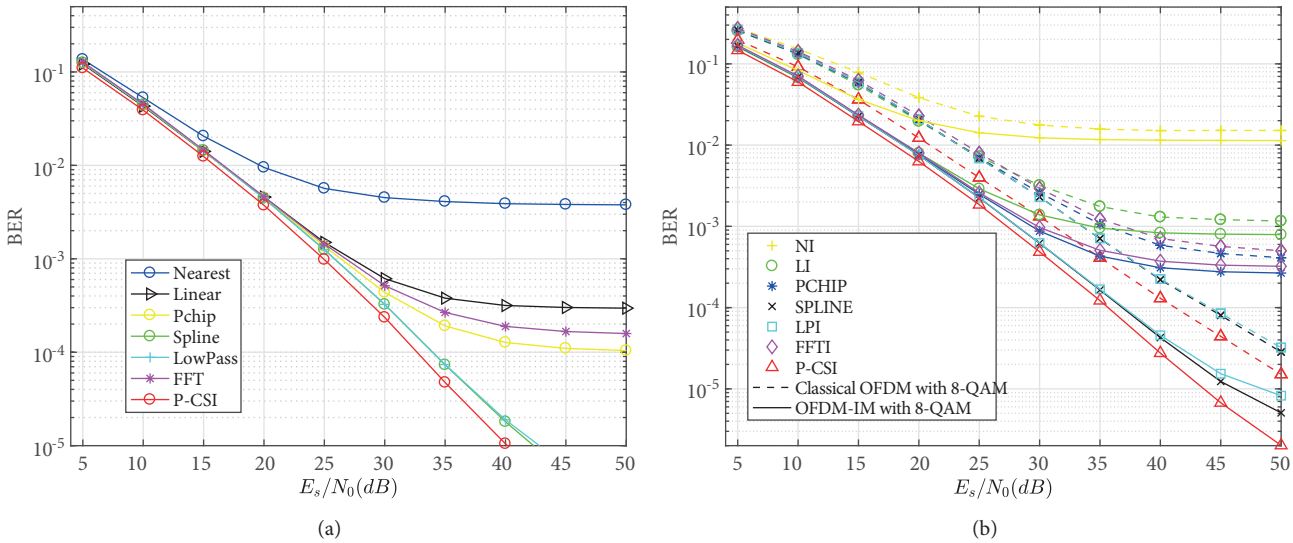

Figure 6. The BER performance of OFDM-IM with $n = 8$, $k = 2$, $PIR = 9$, $N = 512$: (a) QPSK, (b) 8-QAM.

SPLINE exhibit a detection gain of about 4 dB compared to PCHIP at a BER value of 10^{-3}. Moreover, when compared to classical OFDM systems, as seen in this figure, OFDM-IM is more robust to channel estimation errors.

One of the important issues in wireless communications systems is bandwidth efficiency. In [25], it was demonstrated that QAM is very sensitive to channel estimation errors and the performance degradation of a higher order QAM signaling scheme such as 16-QAM is more serious than that of lower order QAM signaling schemes. In Figures 7a and 7b, the effect of channel estimation on the BER performance of OFDM-IM for 16-QAM with $n = 4$, $k = 2$, and $PIR = 9$ is plotted. In Figure 7a, it is shown that NI, PCHIP, PLI, and FFTI experience severe performance degradation at higher SNR values compared to Figures 6a and 6b because of the

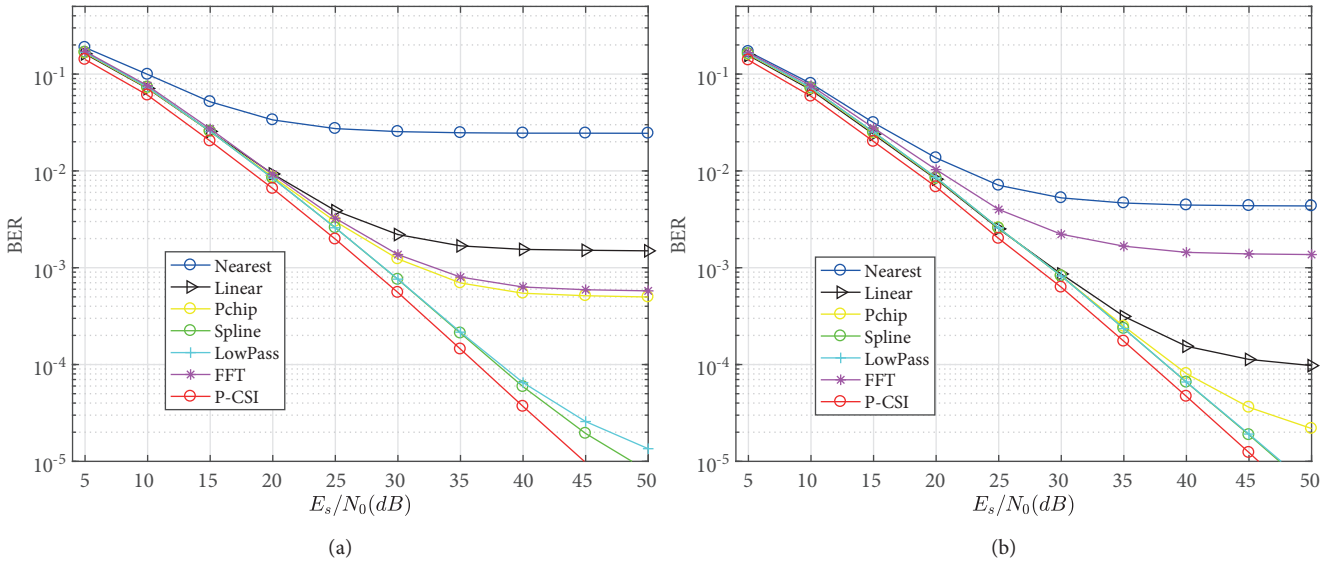

Figure 7. The BER performance of OFDM-IM with 16-QAM, $n = 8$, $k = 2$, $PIR = 9$: (a) $N = 512$, (b) $N = 1024$.

higher order QAM scheme. On the other hand, we increase the number of subcarriers to $N = 1024$ in Figure 7b. It is observed that the BER performance of the SPLINE and LPI-based channel estimator is fairly close to that of the PCHIP-based channel estimator while others also yield error floors at high SNR values. Moreover, the performance difference between interpolation techniques increases as we consider higher modulation formats.

The BER performance results of OFDM-IM with 8-QAM and 16-QAM signaling for parameters $n = 8$, $PIR = 9$, and $N = 512$ at SNR$= 50$ dB are given in Figures 8a and 8b as a function of the activated subcarriers k. It is demonstrated that the BER performance of the OFDM-IM method gets worse while the total number of active subcarriers increases, in parallel with the performance of the channel estimation, which also gets worse. In particular, in Figure 8b, it is observed that LPI and SPLINE have BER values of approximately 10^{-5} while others have higher than 5×10^{-3} for $k = 5$. Consequently, LPI and SPLINE provide more than 500 times better BER values compared to the others.

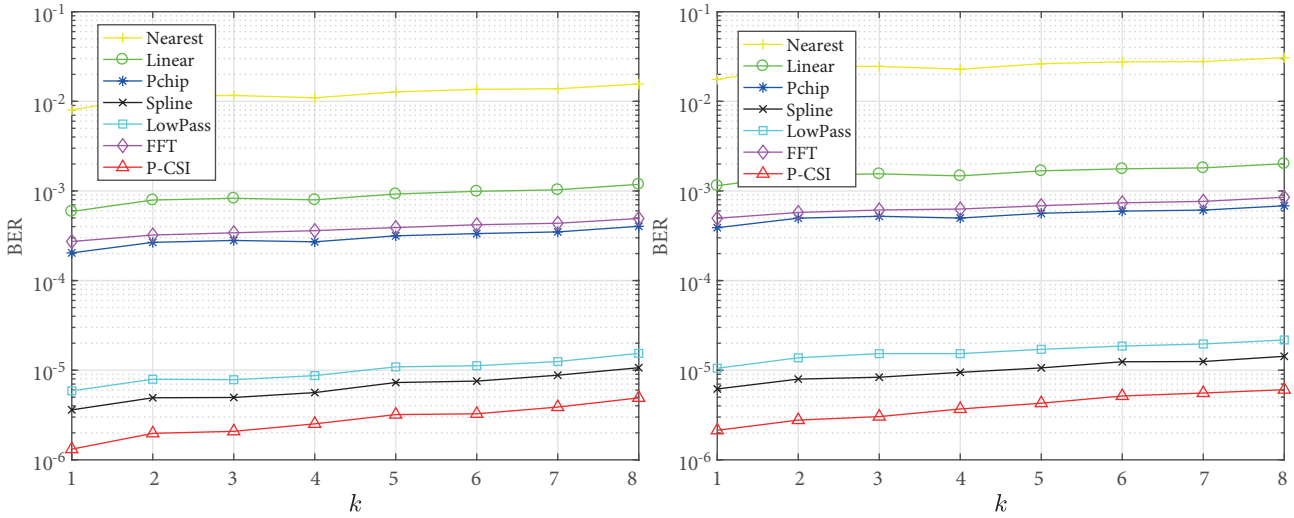

Figure 8. The BER performance of OFDM-IM with $SNR = 50$ dB, $n = 8$, $PIR = 9$: (a) 8-QAM (b) 16-QAM.

The average MSE performance of the proposed channel estimation methods is illustrated in Figures 9a and 9b for OFDM-IM with parameters $k = 2$ and $N = 512$ for a wide range of SNR values. As shown in Figure 9a, the MSE performances of NI, PLI, FFTI, and PCHIP exhibit error floors at high SNR values. Moreover, the MSE performance of LPI is fairly close to that of SPLINE for $n = 4$ and $PIR = 5$. In Figure 9b, it is shown that lower pilot tones (i.e. increasing PIR) cause more MSE performance loss. As a result, the BER and MSE performance results of SPLINE and LPI-based channel estimation techniques indicate that they would be better suited for the OFDM-IM system, which can be considered for next-generation wireless communication systems.

6. Conclusions

In order to detect the OFDM-IM symbols coherently, the implementation of low-complexity, accurate, and efficient channel estimation algorithms for OFDM-IM receivers is an important task. In this work, we have proposed a channel estimation algorithm based on interpolation for OFDM-IM systems operating over frequency-selective Rayleigh fading channels. We also demonstrated the effects of OFDM-IM parameters such as n, k,

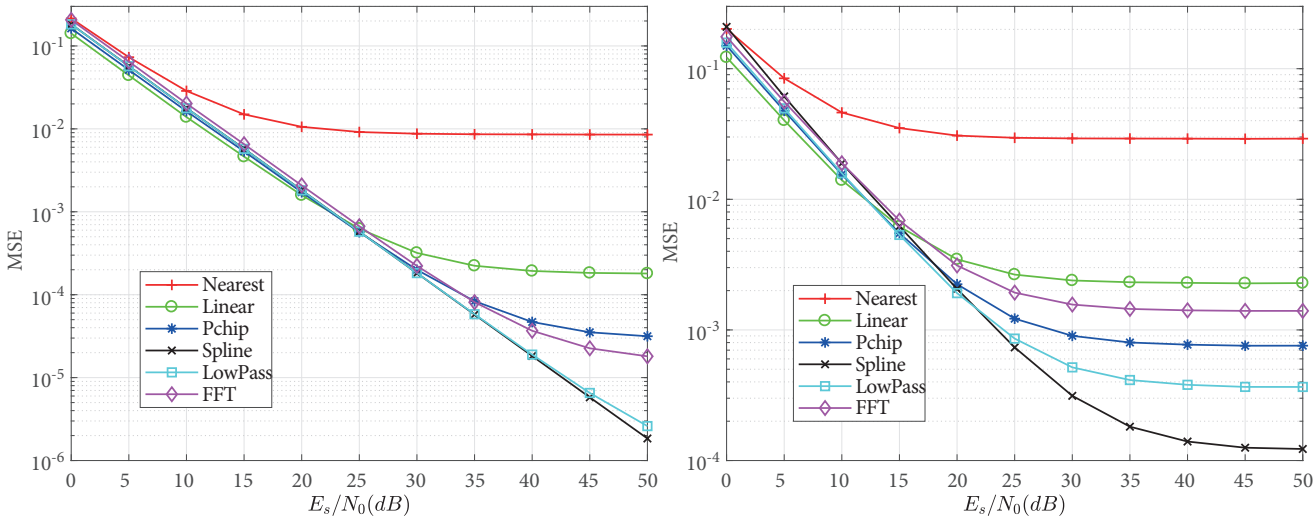

Figure 9. The MSE performance of OFDM-IM with 16-QAM and $k = 2$: (a) $n = 4$, $PIR = 5$; (b) $n = 8$, $PIR = 9$.

and N on the performance of the channel estimation algorithm. It has been shown that the proposed PSA-CE with LPI and SPLINE methods employed in OFDM-IM systems has superior MSE and BER performances in the presence of Rayleigh fading channels compared to PSA-CE with NI, PLI, FFTI, and PCHIP.

Acknowledgments

The work of the first author was supported by the Scientific and Technological Research Council of Turkey (TÜBİTAK) under the BIDEB-2219 Postdoctoral Research Program. The work of the third author was supported by the Turkish Academy of Sciences Outstanding Young Scientist Award Program (TÜBA-GEBİP).

References

[1] Mesleh R, Haas H, Ahn CW, Yun S. Spatial modulation - A new low complexity spectral efficiency enhancing technique. In: Communication and Networking Conference; China; 2006. pp. 1-5.

[2] Shiu D, Foschini G, Gans M, Kahn J. Fading correlation and its effect on the capacity of multi element antenna systems. IEEE Transactions on Communications 2000; 48 (3): 502-513.

[3] Loyka S, Tsoulos G. Estimating MIMO system performance using the correlation matrix approach. IEEE Communications Letters 2002; 6 (1): 19-21.

[4] Sanayei S, Nosratinia A. Antenna selection in MIMO systems. IEEE Communications Magazine 2004; 42 (10): 68-73.

[5] Basar E, Aygolu U, Panayirci E, Poor HV. Orthogonal frequency division multiplexing with index modulation. IEEE Transactions on Signal Processing 2013; 61 (22): 5536-5549.

[6] Basar E. Index modulation techniques for 5G wireless networks. IEEE Communications Magazine 2016; 54 (7): 168-175.

[7] Basar E, Wen M, Mesleh R, Di Renzo M, Xiao Y et al. Index modulation techniques for next-generation wireless networks. IEEE Access 2017; 5 (1): 16693-16746.

[8] Acar Y, Dogan H, Panayirci E. On channel estimation for spatial modulated systems over time-varying channels. Digital Signal Processing 2015; 37: 43-52.

[9] Acar Y, Dogan H, Basar E, Panayirci E. Interpolation based pilot-aided channel estimation for STBC spatial modulation and performance analysis under imperfect CSI. IET Communications 201; 10 (14): 1820-1828.

[10] Acar Y, Dogan H, Panayirci E. Pilot symbol aided channel estimation for spatial modulation-OFDM systems and its performance analysis with different types of interpolations. Wireless Personal Communications 2017; 94 (3): 1387-1404.

[11] Andrews JG, Ghosh A, Muhamed R. Fundamentals of WiMAX: Understanding Broadband Wireless Networking. Edinburgh, UK: Pearson Education, 2007.

[12] Dahlman E, Parkvall S, Skold J. 4G: LTE/LTE-Advanced for Mobile Broadband. San Diego, CA, USA: Academic Press, 2013.

[13] Coleri S, Ergen M, Puri A, Bahai A. Channel estimation techniques based on pilot arrangement in OFDM systems. IEEE Transactions on Broadcasting 2002; 48 (3): 223-229.

[14] Hsieh M, Wei C. Channel estimation for OFDM systems based on comb-type pilot arrangement in frequency selective fading channels. IEEE Transactions on Consumer Electronics 1998; 44 (1): 217-225.

[15] Dyer S, Dyer J. Cubic-spline interpolation 1. IEEE Instrumentation and Measurement Magazine 2001; 4 (1): 44-46.

[16] Dyer S, He X. Cubic-spline interpolation: Part 2. IEEE Instrumentation and Measurement Magazine 2001; 4 (2): 34-36.

[17] Kahaner D, Moler C, Nash S. Numerical Methods and Software. Englewood Cliffs, NJ, USA: Prentice Hall, 1989.

[18] Fritsch F, Carlson R. Monotone piecewise cubic interpolation. SIAM Journal of Numerical Analysis 1980; 17 (2): 238-246.

[19] Boor C. A Practical Guide to Splines. New York, NY, USA: Springer Verlag, 1978.

[20] Coleri S, Ergen M, Puri A, Bahai A. A study of channel estimation in OFDM systems. In: IEEE Vehicular Technology Conference; Vancouver, Canada; 2002. pp. 894-898.

[21] IEEE Acoustics and Speech and Signal Processing Society. Programs for Digital Signal Processing. New York, NY, USA; IEEE Press, 1979.

[22] Singhal K, Vlach J. Interpolation using the fast Fourier transform. Proceedings of the IEEE 1972; 60 (12): 1558-1558.

[23] Fraser D. Interpolation by the FFT revisited-an experimental investigation. IEEE Transactions on Acoustics, Speech, and Signal Processing 1989; 37 (5): 665-675.

[24] Sipila T, Wang H. Time-domain interpolated channel estimation with noise suppression for multicarrier transmissions. In: Eighth IEEE International Symposium on Spread Spectrum Techniques and Applications; Sydney, Australia; 2004. pp. 462-466.

[25] Xia B, Wang J. Effect of channel-estimation error on QAM systems with antenna diversity. IEEE Transactions on Communication 2004; 52 (12): 2209-2209.